

## Verification Test and Model Updating for a Nuclear Fuel Rod with Its Supporting Structure

Heung Seok Kang\*, Kyung Ho Yoon, Hyung Kyu Kim, Kee Nam Song, Youn Ho Jung

Korea Atomic Energy Research Institute  
Dukjin-dong 150, Yusung-Ku, Daejeon 305-353, Korea

### Abstract

*The pressurized water reactor(PWR) fuel rods, which are continuously supported by a spring system called a spacer grid(SG), are exposed to reactor coolant at a flow velocity up to 6~8 m/s. It is known that the vibration of a fuel rod is generated by the coolant flow, a so-called flow-induced-vibration(FIV), and the relative motion incited by the FIV between the fuel rod and SG might wear away the surface of the fuel rod, which occasionally leads to its fretting failure. It is, therefore, important to understand the vibration characteristics of the fuel rod and reflect that in its design. In this paper, the vibration analyses of the fuel rod with two different SGs have been performed by both analytical and experimental methods. The updating of the finite element(FE) model using the measured data has been made in order to enhance the confidence of the FE model of the fuel rod supported by the SG. It was found that the modal parameters are very sensitive to the spring constant of the SG.*

### 1. Introduction

A PWR fuel rod(FR) continuously supported by several SGs As shown in Fig. 1, is exposed to reactor coolant at a flow velocity up to 7 m/s. The coolant flow produces energy to induce vibrations in the FRs, which may result in structural damage. Since the coolant normally flows parallel to the rods, the vibration is called an axial-flow-induced vibration. It is widely accepted that the primary excitation mechanism is the randomly fluctuating pressure acting on the surface of the rods, and this constitutes the excitation force field[1]. The FR extracts energy from the stochastic force field and vibrates predominantly in its lower few modes. The relative motion between the FR and SG induced by FIV is the root cause of fretting wear damage of the FR.

The inside of the FR is pressurized by helium gas up to 26 bars to prevent it from being crushed by a high coolant pressure of 150 bars in the reactor. The internal pressure of the FR in the reactor increases due to fission gases released from the UO<sub>2</sub> pellets in it as burnup increases. Therefore, the FRs are subjected to

tension in the air and to compression after being loaded into the reactor, which gradually decreases as burnup increases.

Since the slenderness ratio( $L/D$ ) of the FR is so big, it is generally considered as the Euler-Bernoulli(E-B) beam multiply supported by several SG and subjected to an axial force. Generally speaking, there are two springs and four dimples whose stiffnesses are much larger than those of the two springs, within a single cell of the SG as shown in Fig. 2.

It is known that the number of SG per fuel assembly(FA) and the spring constants have a significant effect on the modal parameters of the FR. An increment of the number of SG is good in the viewpoint of the decrease of the vibration amplitude of the FR because it makes the span length(length between SGs) short, and the boundary condition of the FR stiff. However, that is restricted due to negative effects to the thermal/hydraulic parameters like pressure drop and heat transmittal. Therefore, the spring constant is the only parameter to control in the development and design of the SG. Strictly speaking, however, even the establishment of the spring constant is limited within some range from the viewpoint of radiation effects.

In this paper, the modal analyses of the FR supported by 5(five) SGs have been performed for two different SGs in numerical and experimental ways. Updating of the finite element(FE) model with the measured data has been made in order to enhance the confidence of the FE model of the fuel rod supported with a SG.

## 2. Finite Element Analysis

For the numerical analysis, a 2-D beam element of ANSYS[2] was used. The frequency range to be calculated was set from 0 to 100 Hz, and modes from 0 to 4. The spring and dimple of the SG were simulated as bent springs. The spring characteristics for both the spring and dimple were obtained by actual tests .

The model geometry and material properties for FE analysis (FEA) are shown in Fig 3.

The higher natural frequencies for the FR with the B type SGs were obtained as compared with those of the A type SGs.

## 3. Modal Test

### (1) Test Setup

The number and position of the accelerometers were determined by the optimal experiment design method which was done by a commercial package (FEMtools)[3]. The optimal measurement points determined are shown in Fig. 4

Pb pellets were inserted instead of  $UO_2$  pellets in the test FR. The test equipment was set as shown in Fig. 4. The impact hammer(or shaker) worked by a trigger input signal. I-STAR was used for data acquisition, and modal analysis was finally performed by FEMtools. Two accelerometers were attached at the one-fourth and three-fourths of a single span of the fuel rod. In addition, one accelerometer was attached on the bed to

monitor noise isolation. Therefore, nine accelerometers were used as shown in Fig. 4. Also, a laser displacement gage was installed in order to check the displacement of the span where the impact hammer(or shaker) worked.

Since the vibration amplitude of the FR in PWR reactor was known to be less than 0.2 mm, 0.5, 1 and 2 N input forces were employed in consideration of that amplitude. The vibration test was performed in air, under cold water and 80 °C hot water

## (2) Test Results

The natural frequencies with the force level obtained by the tests are summarized in Table 1. It was observed that the natural frequencies were apt to decrease with an increase of the force level. It is believed that the FR has nonlinear characteristics with the force level, which was firstly reported by Premount[4]. This phenomenon is believed to be due to the nonlinear characteristics of the spring according to the force level. As expected, the natural frequencies for the FR under cold water decrease due to the so-called added mass effect. However, in hot water (80 °C), the natural frequencies increased more than our expectation that the added mass effect would decrease due to the decrease of water density. It could be explained by the increase of the internal pressure caused by the isovolumetric change of helium gas as the temperature increased. The pressure increased the axial force on the FR, which made the stiffness term strong, and the natural frequencies increased. A bigger displacement of the FR under cold water than in air was observed at the same force level. The displacement of the FR under hot water could not be measured due to vapor, which disturbed the laser displacement gage in operation. Two typical FRFs for the three different environments are shown in Fig. 5 and 6. As mentioned before, nonlinear characteristics can be observed.

## 4. Model Comparison, Sensitivity Analysis and Model updating

### (1) Model Comparison with FEM and Experiment

Since the FR has a uniform mass per length, and its dimensions are strictly controlled while manufacturing, structural modification on the mass or stiffness term is meaningless. It is known that the dynamic behavior of the FR is significantly influenced by the characteristics of the SG spring and dimple, and whether the dimple exists or not. For this reason, sensitivity studies and modification have been performed regarding the spring constants for both the spring and dimple. An accurate FE model of the FR requires the accurate simulation of spring boundary conditions.

In order to find out and modify the difference of the dynamic characteristics between experimental and FE model, mode pairing was done by the well-known Modal Assurance Criteria(MAC) equation as follows:

$$MAC(\Psi_i, \Psi_j) = \frac{|\Psi_i^T \Psi_j|^2}{(\Psi_i^T \Psi_i)(\Psi_j^T \Psi_j)} \quad (1)$$

A comparison with experimental analysis (EMA) and FEA on the FR with A and B type SG is shown in Table 2. The MAC analysis result for the A type SG is representatively depicted in Fig. 7.

Three(3) modes have been identified for the FR with the both SG. The discrepancy of the 1<sup>st</sup> natural frequency is large between FEA and EMA with the A type SG, while relatively good agreement was obtained with the B type SG.

Each mode shape for the FR with both SG reveal the same pattern as shown in Fig. 8.

## (2) Sensitivity Analysis

The discrepancy of the 1<sup>st</sup> natural frequency between FEA and EMA was so big for the FR supported by the A type SG. Sensitivity analysis on the SG spring and dimple was performed by the following equations for the A type SG prior to updating of the FE model

$$\frac{\partial \{\mathbf{f}_i\}}{\partial p_j} = \sum_{k=1}^N a_k^i \{\mathbf{f}_k\} \quad (2)$$

$$a_k^i = \frac{\{\mathbf{f}_i\}^T \left( \frac{\partial [K]}{\partial p_j} - \mathbf{I}_i \frac{\partial [M]}{\partial p_j} \right) \{\mathbf{f}_k\}}{\mathbf{I}_i - \mathbf{I}_k} \quad (3)$$

It is impossible to have such a large difference between FEA and EMA due to mass or stiffness inconsistency, but possible to have it due to the stiffness discrepancy of the SG spring or dimple. The sensitivity analysis results according to the mode shapes are shown in Fig. 9 for the A type SG. Five springs were represented as parameters 1 through 5, and ten dimples as 6 through 15. The stiffness of the dimple in the SG has been more sensitive to the dynamic characteristics of the FR than that of the spring.

## (3) Model Updating

Model updating is a process to improve an FE model of a structure using measured dynamic data from the same structure. Over the past decade or so a number of updating techniques have been proposed. A review of the different methods can be found in reference 5. The cost function that should be minimized has been defined as follows:

$$\Omega = [\{R_e\} - \{R_a\}]^T [C_R] [\{R_e\} - \{R_a\}] + [\{P_e\} - \{P_a\}]^T [C_P] [\{P_e\} - \{P_a\}] \quad (4)$$

Where, R: Structural Response (a: analysis, e: experiment)

P: Parameter (a: analysis, e: experiment)

C: Weight Function of Response (R: response, P: Physical)

As mentioned, the same weighting was imposed for physical quantities( $C_p$ ) such as mass and stiffness of the FR, however, higher weighting was put to the lower modes since the lower mode was known to give the higher contribution to the vibration. The model updating results are summarized in Table 3. The effect of the soft middle spring on model improvement was insignificant compared with dimples. The model updating process drastically decreased the stiffnesses of the dimples in the 2<sup>nd</sup> and 3<sup>rd</sup> SG. The decrease of the cost function has turned out to be insignificant after the 1<sup>st</sup> iteration. Comparisons of natural frequencies between before and after model updating are shown in Table 4, which shows their good agreement.

## 5. Conclusions and Discussion

Vibration analyses of a fuel rod supported by two different SGs have been performed by both analytical and experimental methods. The updating of the FE model of the FR with an A type SG using the measured data was performed to enhance the confidence of the FE model. Since the fuel rod has well-controlled mass per length and stiffness, sensitivity analysis and model updating have been made on the support spring constant. It was found that the modal parameters (natural frequency and mode shape) are very sensitive to the dimple stiffness of the SG. Dimple stiffness is much higher than that of the spring. Therefore, the dimple can have more effect on the stiffness matrix than the spring. For this reason, it is explained that the dimple is more sensitive than the spring to dynamic characteristics of the FR. However, since the SG was manufactured under well-controlled conditions, it is impossible to physically explain such a large decrease of the spring constant of a dimple. The lower natural frequencies from EMA were believed to be partially due to the nonlinear characteristics of the spring, mainly mal-supporting condition like the existence of some gap between the FR and dimple while vibrating. The fact that the gap between the FR and SG exists is the worst manufacturing condition because it is well known that such a gap easily accelerates fretting wear on the FR during operation, which consequently leads to failure of the FR. Collective action should be taken prior to loading the FR into a reactor. Although the model update technique was originally aimed to enhance the reliability of the FE model, for a system like a nuclear FR the technique can be employed during manufacturing to identify if the FR is well supported by the SG or not.

### **Acknowledgement**

This project has been carried out under the nuclear R&D program by MOST.

### **References**

1. M. P. Paidoussis, Fluidelastic Vibration of Cylinder Arrays in Axial and Cross Flow, *J. of Sound and Vibration*, Vol. 76, pp. 329-360, 1981.
2. ANSYS, Users Manual Version 5.3.
3. FEMtools, Users Manual Version 1.4.
4. A. Premount, "On the Vibrational Behavior of Pressurized Water Reactor Fuel Rods", *Nuclear Technology*, Vol. 58, pp. 483-491, 1982.
5. Friswell, M. I. Mottershead, J. E., *Finite Element Model Updating in Structure Dynamics*, Kluwer Academic Publishers, 1995.

Table 1 Natural Frequency and Displacement Comparison According to Force (in-air)

Force Level	Type Mode	In-air		Cold Water		Hot Water(80°C)	
		A	B	A	B	A	B
0.5 N	1 <sup>st</sup> mode (Hz)	35.2	44.4	33.7	42.5	33.9	44.7
	Disp. (mm)	0.05	0.016	0.07	0.019	-	-
1.0 N	1 <sup>st</sup> mode (Hz)	33.6	40.6	31.5	40.2	32.4	42.5
	Disp. (mm)	0.098	0.040	0.113	0.053	-	-
2.0 N	1 <sup>st</sup> mode (Hz)	30.7	37.4	28.8	37.5	29.5	39.8
	Disp. (mm)	0.196	0.106	0.229	0.134	-	-

Table 2 Comparison with FE Analysis and Experimental Results for A Type SG

Mode No	A TYPE				B TYPE			
	FEA	EXP	Error (%)	MAC (%)	FEA	EMA	Error(%)	MAC(%)
1	43.9	35.2	24.69	83.2	42.9	44.4	-3.24	88.8
2	48.3	46.4	4.14	55.4	47.6	50.5	-5.82	59.5
3	53.8	49.2	9.45	94.8	53.5	52.3	2.35	92.6

Table 3 Model Updating Results for Spring Constant vs. Iteration No. (S-Spring, D-Dimple)

No	Type	Model Value	1 <sup>st</sup> Tune	2 <sup>nd</sup> Tune	3 <sup>rd</sup> Tune	No	Type	Model Value	1 <sup>st</sup> Tune	2 <sup>nd</sup> Tune	3 <sup>rd</sup> Tune
1	S	1.53E5	1.53E5	1.53E5	1.53E5	9	D	8.84E6	6.41E5	5.78E5	5.24E5
2	“	1.53E5	1.53E5	1.53E5	1.53E5	10	“	8.84E6	1.77E6	1.83E6	1.93E6
3	“	1.53E5	1.53E5	1.53E5	1.53E5	11	“	8.84E6	2.58E6	2.84E6	3.14E6
4	“	1.53E5	1.53E5	1.53E5	1.53E5	12	“	8.84E6	6.98E6	6.86E6	6.64E6
5	“	1.53E5	1.53E5	1.53E5	1.53E5	13	“	8.84E6	7.91E6	8.09E6	8.09E6
6	D	8.84E6	5.79E5	5.62E6	5.47E6	14	“	8.84E6	1.06E7	1.17E7	1.8E6
7	“	8.84E6	5.08E5	4.85E6	4.64E6	15	“	8.84E6	1.02E7	1.1E7	1.05E6
8	“	8.84E6	1.38E6	1.4E6	1.41E6	-	-	-	-	-	-

Table 4 Comparison of FE Analysis with Before and After Model Updating

Mode No	After(Hz)	Before(Hz)	Error(%)	MAC(%)
1	35.5	35.2	0.89	76.5
2	44.64	46.4	-3.70	44.1
3	52.8	49.2	7.44	95.9
4	88.9	88.6	0.33	55.2

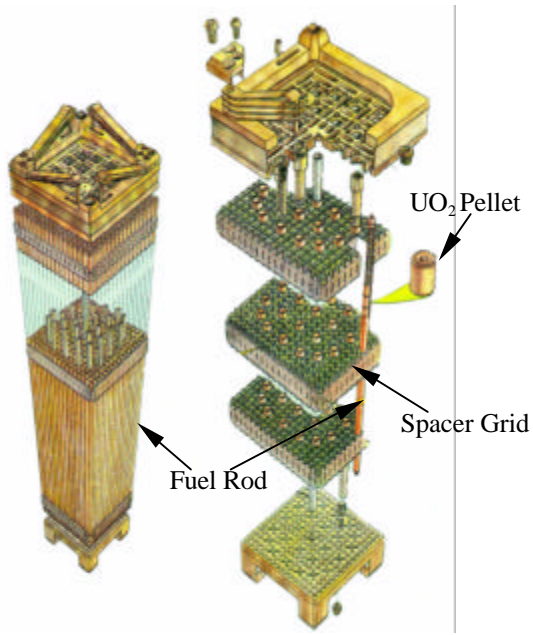


Fig. 1 Fuel Rods in PWR Fuel Assembly

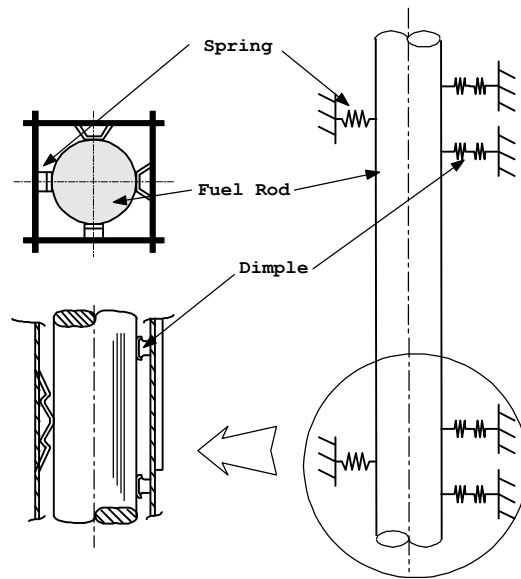


Fig. 2 Fuel Rod Model with Spacer Grids

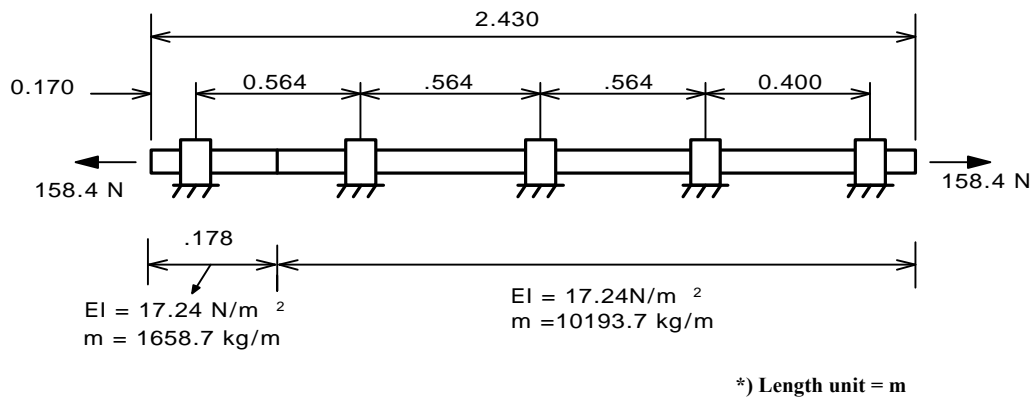


Fig. 3 Geometry and Material Properties for the FR Model

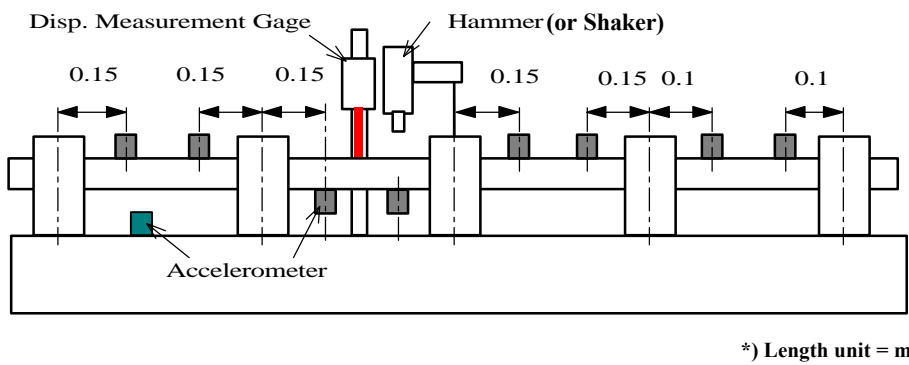


Fig. 4 Test Setup

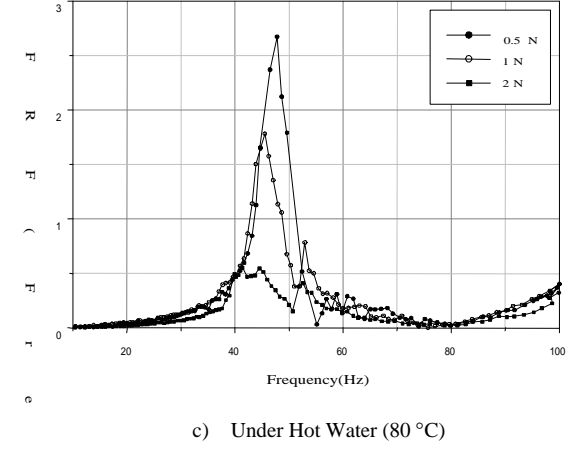
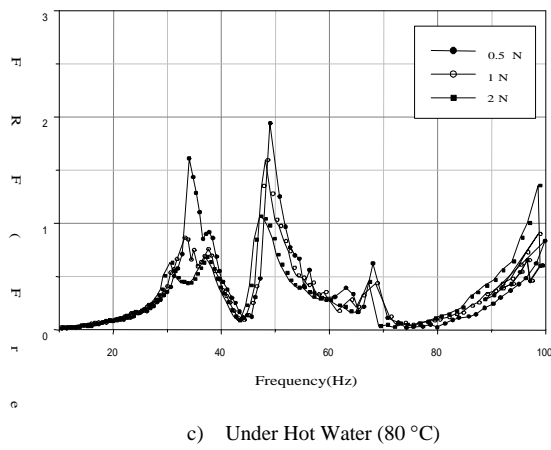
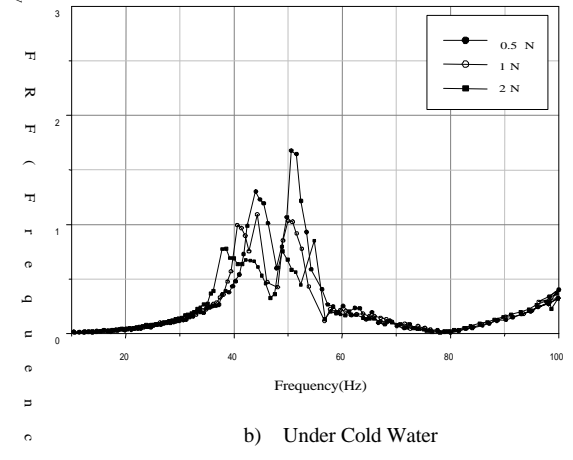
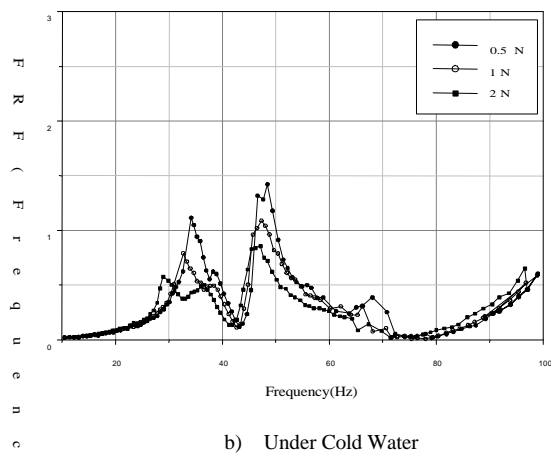
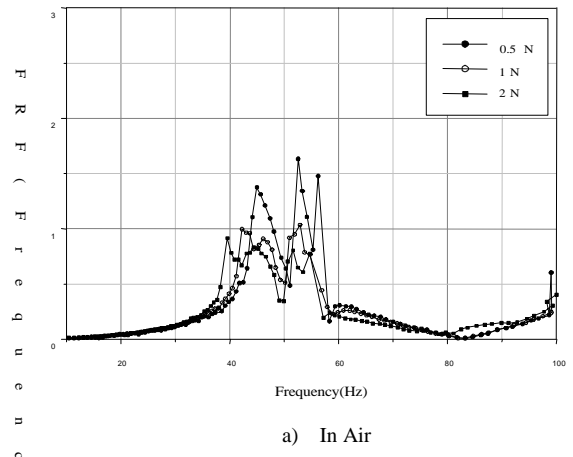
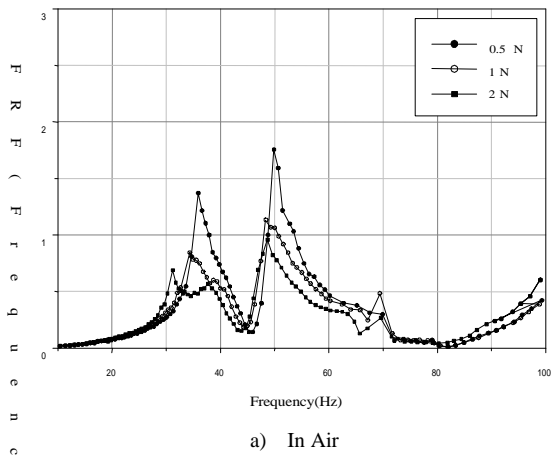


Fig. 5 FRFs for the FR with SG Type A

Fig. 6 FRFs for the FR with SG Type B



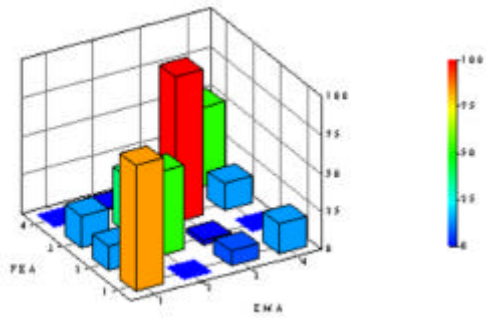


Fig. 7 MAC Comparison for A Type SG

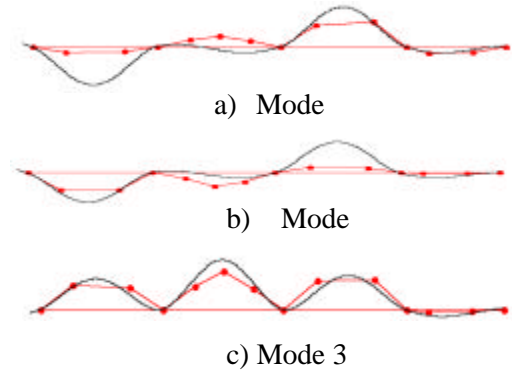


Fig. 8 Mode Shapes of FR with A Type SG

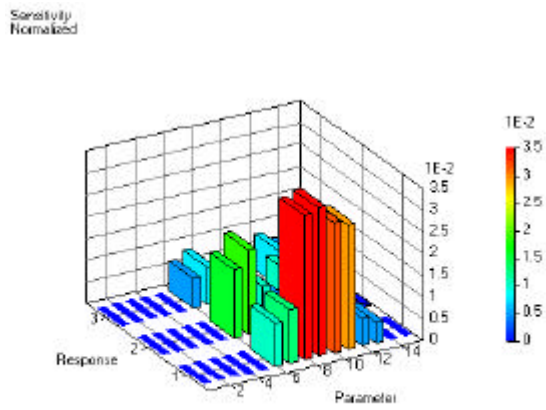


Fig. 9 Sensitivity Comparison for Spring and Dimple Stiffness of A Type SG